DOI: 10.1002/ejic.200501009

Phase Relations Between β-Tricalcium Phosphate and Hydroxyapatite with Manganese(II): Structural and Spectroscopic Properties

Isaac Mayer,*[a] Frederic J. G. Cuisinier,[b] Ina Popov,[c] Yechezkel Schleich,[a] Sarit Gdalya,[a] Olaf Burghaus,[d] and Dirk Reinen[d]

Keywords: Manganese / β-Tricalcium phosphate / EPR spectroscopy

The preparation of Mn-containing β-tricalcium phosphate (β-TCP) samples was achieved in two ways: a) transformation of precipitated Mn-containing calcium hydroxyapatite (HA) to β-TCP by heating at 1100 °C, and b) preparation by solid-state reaction of a mixture of $CaCO_3$, $(NH_4)_2HPO_4$, and $Mn(NO_3)_2$ at 1100 °C. Powder X-ray diffraction (XRD) analyses of the samples, obtained by both methods, show well-defined patterns with structural data of the rhombohedral R3c, β-TCP phase. The calculated lattice constants are smaller than those known for β-$Ca_3(PO_4)_2$ because of substitution of Ca^{2+} by Mn^{2+}. EPR spectroscopy indeed reveals that manganese is divalent in the samples. Apparently, the Ca(5) site in the β-TCP structure is occupied by Mn^{2+}. The distribution of Mn^{2+} between the β-TCP and the HA phase in the case of preparation (b) was studied by EPR spectroscopy, and a pronounced preference for the former lattice was found. Micron- and submicron-sized crystals with visible faces were observed by TEM in the case of β-TCP prepared by solid-state reaction, and large micron-sized, droplike-shaped crystals, sensitive to beam radiation, were found in the case of samples prepared by heating HA at elevated temperatures.

Introduction

Calcium hydroxyapatite (HA), the main constituent of bones and teeth, is biocompatible and widely used in dentistry and orthopedics to repair bone defects and substitution, and as coating material for metallic implants. β-Tricalcium phosphate is also known as a biocompatible material and is found in many cases to be advantageous as compared with HA.[1–3] It is also used as a host when doped with Mg, Zn, and Cd ions.[4,5]

In previous work,[6] HA samples containing Mn^{2+} were prepared by a precipitation method. The motivation for the addition of Mn^{2+} ions to HA was due to the fact that divalent Mn^{2+} has been linked to the activation of integrins,[7] a family of receptors that mediate cellular interactions with extracellular matrix and cell surface ligands. In the presence of Mn^{2+} ions the ligand affinity of integrin increases and cell adhesion is promoted. High-temperature treatment of the precipitated samples showed that samples with low carbonate content transform partially or completely to β-TCP. EPR spectroscopy proved that manganese is divalent also in the heated samples and is found to partly occupy Ca^{2+} sites in the β-TCP structure.[6] In further work,[8] human osteoblasts were cultured on the surfaces of Mn-doped HA thin films deposited on etched Ti substrates. Biological tests demonstrated that the Mn-doped HA coatings favor osteoblasts proliferation, activation of their metabolism, and differentiation.

The aim of the present work was to prepare Mn-doped β-TCP samples and to determine the Mn^{2+}/Ca^{2+} miscibility limit. Two preparation methods were applied: a) transformation of Mn-containing HA to β-TCP, and b) preparation of β-TCP by high-temperature solid-state reaction of stoichiometric mixtures of $CaCO_3$, $(NH_4)_2HPO_4$, and $Mn(NO_3)_2$.

Results

β-TCP Prepared by Heating Precipitated HAMn

HAMn samples were prepared with a broad range of Mn content (0.1–4.0%). In Table 1, Mn content and Ca/P molar ratios of the samples are listed. The Ca/P values of the original HAMn samples were always lower than 1.67, indicating nonstoichiometric HA, and these values decreased with increased Mn content. The powder XRD patterns of the precipitated HAMn samples had reflections solely of the hexagonal apatite structure. The XRD patterns of the samples after heating to 400 °C showed no change in their crystal structure. At 600 °C the XRD patterns already contained

[a] Department of Inorganic and Analytical Chemistry, Hebrew University,
Jerusalem 91904, Israel
[b] INSERM U 424, Centre de Recherches Odontologique,
1 Place de l'Hospital, 6700 Strasbourg, France
[c] Unit Nanoscopic Characterization, Hebrew University,
Jerusalem 91904, Israel
[d] Fachbereich Chemie und Zentrum für Materialwissenschaften, Philipps Universität,
35032 Marburg, Germany

Table 1. β-Tricalcium phosphate phases obtained by heating HAMn samples to 800–1000 °C. Lattice constants and unit cell volumes, Mn content, Ca/P molar ratios (in the initial HA phase), and estimated rates of transformation to β-TCP.

Sample	Mn (1)[a] molar content	Lattice constants [Å] *a*	*c*	Lattice volume [Å^3]	Ca/P molar ratios	Transformation to β-TCP [%]
$Ca_3(PO_4)_2$	–	10.43	37.38	3522	1.50	–
HAMn28	0.030	10.42	37.37	3510	1.54	65
HAMn5b	0.035	10.42	37.35	3510	1.49	85
HAMn147	0.070	10.41	37.33	3505	1.48	65
HAMn142	0.105	10.40	37.29	3494	1.48	70
HAMn145	0.117	10.39	37.25	3482	1.51	75
HAMn146	0.130	10.39	37.20	3478	1.45	75
HAMn149	0.150	10.39	37.24	3483	1.41	75
HAMn158	0.165	10.30	37.29	3473	1.41	75

[a] (1) in β-TCP, if complete transformation would occur.

reflections of two crystal phases: reflections of the original hexagonal HA phase[9] and reflections of the rhombohedric β-TCP.[10] In the 800–1000 °C region, most of the HA (around 75%) transformed to β-TCP. The degree of transformation of HA to β-TCP was roughly estimated by the relative peak heights of the strongest HA (211) and β-TCP (0.2.10) reflections. These findings suggest that the hexagonal apatite structure of the nonstoichiometric HA samples is stable even at very low Ca/P ratios and transforms to the rhombohedral structure only on heating. The structural data of the rhombohedral phases are listed in Table 1.

β-TCP Prepared by Solid-State Reaction

Samples with a general composition of $Ca_{3-x}Mn_x(PO_4)_2$ were prepared with different x values in the range of 0.1–1.0 in intervals of 0.1 and appear in Table 2. The XRD patterns of the obtained samples revealed that these samples crystallize in the R3c rhombohedral structure characteristic of β-TCP. No reflections of a different impurity phase were present up to the composition $Ca_{2.4}Mn_{0.6}(PO_4)_2$. Above this composition the XRD pattern contained peaks of a second unknown crystal phase. Apparently, about 20 mol-% of Mn^{2+} can be substituted for Ca^{2+} in β-TCP.

Table 2. Structural data of β-$Ca_{3-x}Mn_x(PO_4)_2$ solid solutions obtained by solid-state reaction.

Lattice constants [Å] *c*	*a*	Lattice volume [Å^3]	Composition	Samples
37.38	10.431	3522	$Ca_3(PO_4)_2$	TCP
37.37	10.424	3517	$Ca_{2.9}Mn_{0.1}(PO_4)_2$	TCPMn1
37.32	10.404	3498	$Ca_{2.8}Mn_{0.2}(PO_4)_2$	TCPMn2
37.32	10.376	3480	$Ca_{2.7}Mn_{0.3}(PO_4)_2$	TCPMn3
37.31	10.395	3491	$Ca_{2.6}Mn_{0.4}(PO_4)_2$	TCPMn4
37.26	10.366	3465	$Ca_{2.5}Mn_{0.5}(PO_4)_2$	TCPMn5
37.22	10.351	3453	$Ca_{2.4}Mn_{0.6}(PO_4)_2$	TCPMn6

All samples listed in Table 1 and Table 2 were pink at high Mn concentrations and were white at low Mn concentrations. This is in agreement with a +2 oxidation state and hence with the presence of only very weak Laporte- and spin-forbidden transitions in the d-d spectrum of the visible region.

EPR Analysis

Our previously published EPR spectroscopic data showed that precipitated HAMn[6] contains Mn^{II} in the cubic or nearly cubic environment of an impurity phase, presumably $MnCO_3$ or $Mn(OH)_2$. The EPR spectra in Figure 1 show the characteristic six-line hyperfine structure with $A \approx 90$ G (≈ 0.0085 cm^{-1}) at Q-band frequency, without any indication of a zero-field splitting also in the X-band, thus excluding the presence of Mn^{2+} in Ca^{2+} positions. On heating to 600 and 800 °C the samples behaved differently, depending on their carbonate content: carbonate-rich (CR) samples retained the apatite structure, while carbonate-poor (CP) samples transformed partly or fully to the β-TCP type.

The Q-band spectrum of Mn^{2+}-doped β-TCP prepared by high-temperature solid-state reaction is shown, together with a simulated spectrum with a zero-field splitting of D = 0.047 cm^{-1} (500 G), in Figure 2 (bottom). Besides the partly resolved central signal, whose hyperfine splitting is not accounted for in the simulation (A = 0), the agreement is fairly good, suggesting that the chosen D-parameter is near to the one of the experimental spectrum. Inspecting the crystal structure of β-TCP[11] with its five different Ca positions, it is most likely that Mn^{2+} is substituted into the Ca(5) site. The coordination number (CN) is six, the polyhedron geometry is a slightly hexagonally distorted octahedron with C_3 point symmetry, and Ca–O bond lengths of 2.263(25) Å are much shorter than the average distances in the other polyhedra with CNs between seven and nine (>2.4 Å). The reported Ca(5)–O bond lengths are surprisingly even smaller than those in CaO (2.40 Å) and rather close to those in MnO (2.22 Å),[13] which both crystallize in the NaCl type. Because the symmetry of the $Ca(5)O_6$ polyhedron is axial, a vanishing (orthorhombic) E-parameter is indeed expected in the case of isomorphous substitution of Ca^{2+} by Mn^{2+}. Figure 2 (top) shows, in small size, the spectrum of a CP sample with β-TCP structure as well, but obtained from solution by subsequent heating to 800 °C. It is identical with the bottom spectrum, though less resolved because of a poorer sample crystallinity. It can be concluded, therefore, that Mn is present as Mn^{II} in a Ca^{2+} position of the β-TCP host. The X-band measurement on the same two samples confirms this result (Figure 3). The spec-

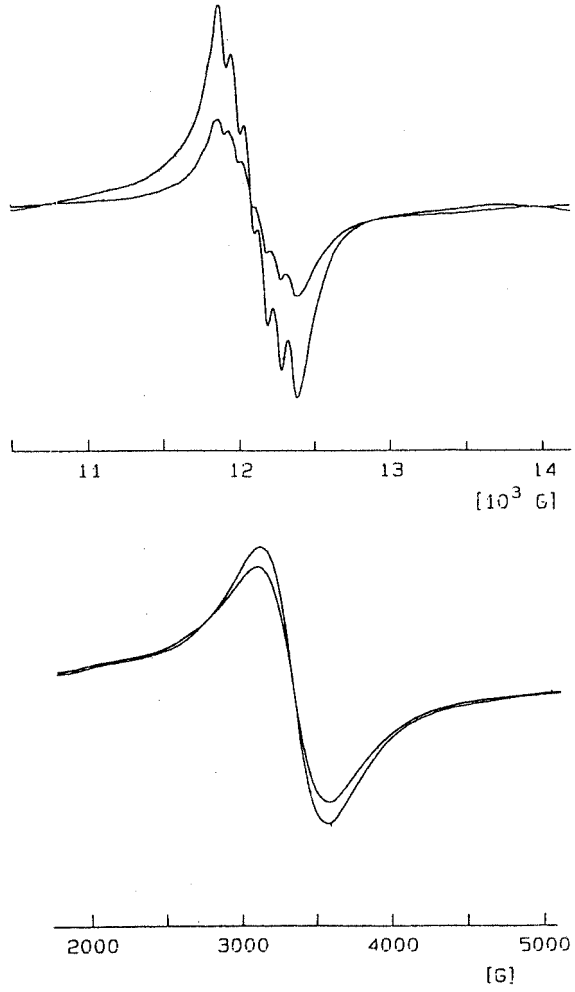

Figure 1. Typical Q- (33.93 GHz) and X-band (9.26 GHz) spectra of precipitated calcium hydroxyapatites in the presence of Mn (298 K).

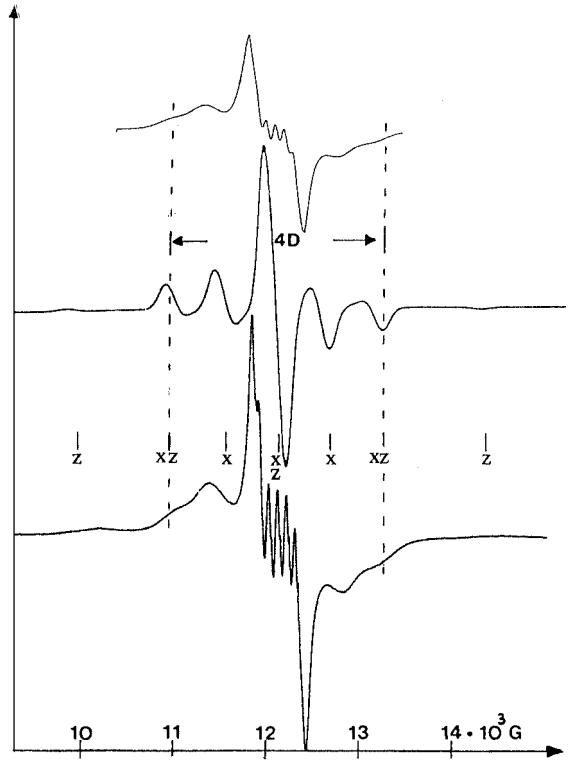

Figure 2. EPR Q-band spectra (34.0 GHz) of Mn^{2+}-doped β-TCP obtained by solid-state reaction (TCPMn1; 126 K, bottom) and from solution after subsequent heating to 800 °C with nearly complete transformation to β-TCP (298 K, top), as compared with a simulated spectrum with $D = 0.047\ cm^{-1}$, $A = 0$ (adopted from ref.[12]). The transition parallel (z) and perpendicular ($x = y$) to the preferred axial direction are indicated.

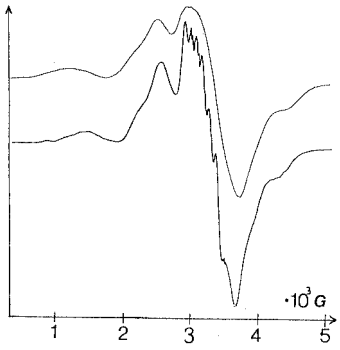

Figure 3. X-band spectra (9.22 GHz; 298 K) of Mn^{2+}-doped β-TCP by solid-state reaction (TCPMn1; bottom) and of a CP sample from solution after subsequent heating to 800 °C (top).

tra are identical, but again with a partly resolved hyperfine structure in the case of the sample obtained by solid-state reaction.

The Q-band EPR spectra (Figure 4) of heated Mn-doped CR samples have a completely different appearance from the one in Figure 2 (top). Each hyperfine line in the central part of these spectra undergoes an increasingly pronounced splitting when raising the temperature; this is obviously mainly caused by better resolution due to an improved sample crystallinity at higher heating temperatures. It corresponds to a tiny zero-field D-parameter of about 0.002 cm^{-1} (≈ 20 G). It is distinctly smaller than A and by far too small to indicate substitution into a Ca^{2+} site in the lattice. The solids turned blue after heating above 400 °C. Very weak features between 8000 and 17000 G (not shown here) and the well-resolved half-field signal (Figure 4, inset) are indicative of this color effect, caused by the formation of Mn^{V} in the tetrahedral P^{V} position of the apatite host, as was substantiated by optical spectroscopy.[6] A rough assignment of the latter resonances is possible with the parameters $D \approx 0.40\ cm^{-1}$, $E \approx 0.05\ cm^{-1}$, and a g-factor of ca. 1.96, values which are near to those of Mn^{V}-doped $Sr_5(PO_4)_3$-Cl.[14] The obvious reason that Mn^{2+} is not substituted into the Ca^{2+} site of the apatite lattice, even after heating to 800 °C, is the weak tendency to occupy Ca^{2+} positions of CNs seven and nine in this structure, at least at moderate heating temperatures. Apparently, the preference of Mn^{2+} to enter a Ca^{2+} position in the two alternative host lattices is much stronger in the case of β-TCP and is supported by ionic size considerations.

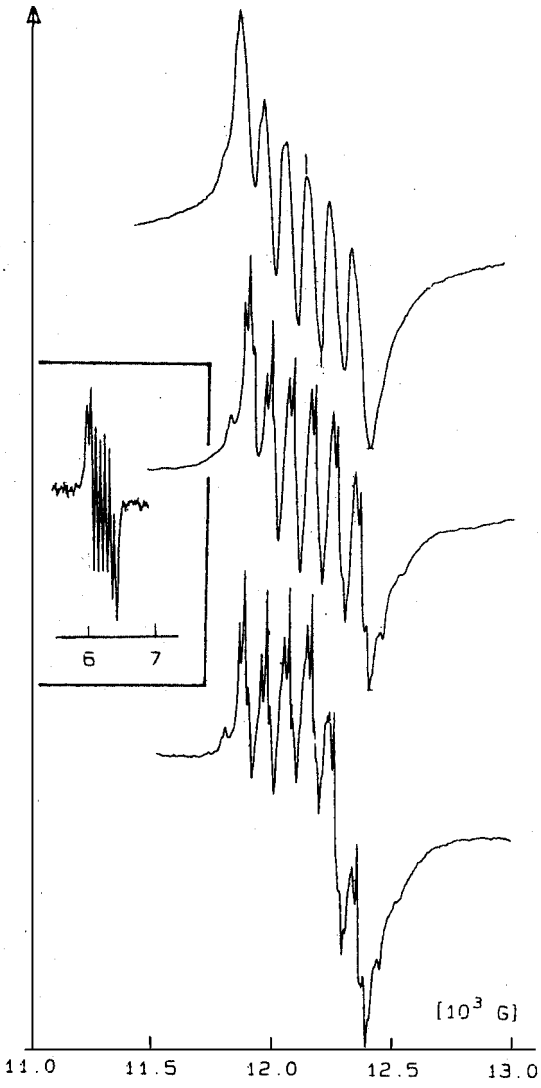

Figure 4. Q-band spectra (34.0 GHz; 298 K) of a CR sample from solution in the presence of Mn, when subsequently heated to 400 °C (top), 600 °C, and 800 °C (bottom). The (enlarged) half-field signal (inset), is due to Mn^{V}.

Considering TCP samples with increased Mn content, the X-band spectrum of TCPMn3 (Table 2, Figure 5) or the very similar spectrum of sample HAMn146 after the heat treatment at 800 °C (Table 1), still show the essential features of TCPMn1 (Figure 3), though the increase in the Mn^{2+} concentration has partly narrowed the signal, as a result of exchange interactions between the d^5 cations in the lattice. However, a striking feature is that a further increase in the Mn concentration far beyond the one which corresponds to the full occupation of the Ca(5) site ($Mn_{0.286}$), completely removes the features characterizing the zero-field splitting (TCPMn6 in Figure 5). This result might be the consequence of the substitution of further Ca^{2+} sites in such a way that neighbored polyhedra to $Mn(5)O_6$ (which lie isolated in the lattice) with common oxygen ligand atoms are involved, inducing intense exchange narrowing in the EPR spectra.

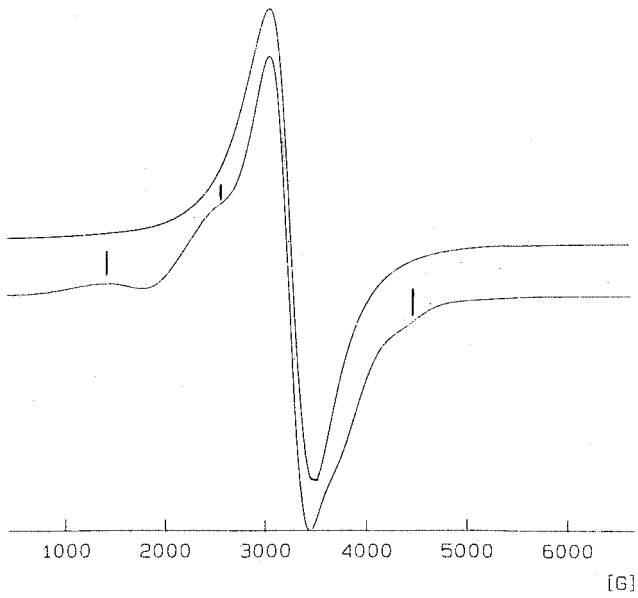

Figure 5. X-band spectra (9.11 GHz; 298 K) of solids TCPMn3 (bottom; the zero-field splitting is marked, see Figure 3) and TCPMn6 (top), with high Mn concentrations (Table 2).

TEM

Two β-TCP samples were analyzed by TEM methods: a sample prepared after heating sample HAMn147, and $Ca_{2.7}Mn_{0.3}(PO_4)_2$ prepared by solid-state synthesis.

The HAMn147 crystals were 3D, rounded, and droplike-shaped (Figure 6). The smallest crystals were 100 nm in size, but in general they were larger, up to tens of microns. The small crystals had a polyhedral shape in most cases, while small round crystals were also observed. The crystals were not transparent enough to see their lattice, but several good

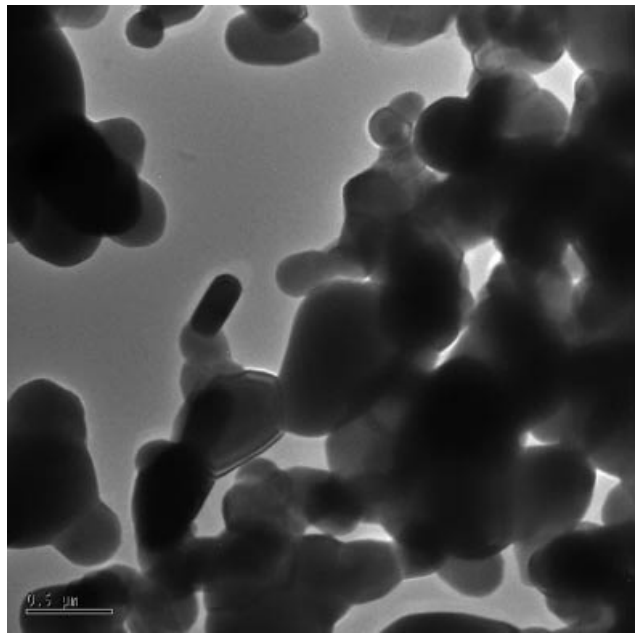

Figure 6. Droplike-shaped crystal of sample HAMn147 after heating to 800 °C.

images of their lattice were still observed. The crystals were extremely sensitive to radiation damage; holes were formed in the crystallites. This most probably indicated that the material was composed of nanometer-sized crystalline flakes, which lost their mutual order under the radiation but did not disappear. Comparison of these results with the TEM results of parent HA[6] shows that after heat treatment the morphology changed from thin platelike polygons to 3D crystals.

In the case of $Ca_{2.7}Mn_{0.3}(PO_4)_2$ two groups of crystallites were observed: 2D polygonal flakes of crystallites of nanometer size (nonstable under radiation) (Figure 7) and large, hundreds of nanometers in size, 3D crystallites which were more stable under radiation. Good lattice images and at least one good electron-diffraction pattern from the big crystallites were obtained.

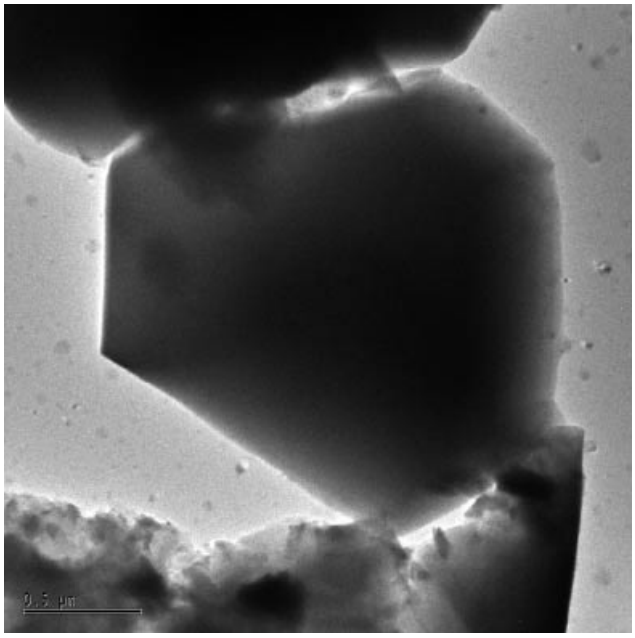

Figure 7. Large 3D crystal of $Ca_{2.7}Mn_{0.3}(PO_4)_2$.

Discussion

The aim of the present work was to prepare Mn-doped β-TCP samples which can be considered as improved biocompatible coating materials for metallic implants. The results of this study reveal that these materials can be prepared either by heating precipitated Mn-containing HA samples above 600 °C, or by solid-state reaction. The low observed Ca/P ratios for the samples with relatively high Mn concentration (Table 1) indicate an enhanced substitution of HPO_4^{2-} anions into the HA lattice, thus generating Ca^{2+} vacancies. This might be caused by the release of H^+ as the consequence of precipitation of some amorphous $MnCO_3$ or $Mn(OH)_2$. Ca/P ratios even below 1.5 favor the transformation to β-TCP in the presence of larger percentages of Mn with the ability to occupy Ca^{2+} positions (see Table 2).

XRD analyses prove that the samples obtained by both methods crystallize in the rhombohedric β-TCP structure; the lattice constants and volumes (hexagonal setting) listed in Table 1 and Table 2 show a slight but continuous decrease with the increase in Mn content. This indicates the formation of solid solutions by partial replacement of Ca^{2+} by the smaller Mn^{2+} ions in the β-TCP lattice. In the case of the precipitated samples, transformation of HA to β-TCP is partial, and a mixture of HA and β-TCP is always obtained; the maximum transformation, about 75%, is reached at 800 °C. Such mixtures are actually often recommended for coating purposes. In the solid-state reaction, the product is of the rhombohedric β-TCP crystal phase only, with maximum Mn content of the composition $Ca_{2.4}Mn_{0.6}(PO_4)_2$.

The unit cell parameters of the $Ca_{3-x}Mn_x(PO_4)_2$ series indicate a discontinuity around $x = 0.3$, which is in well agreement with EPR spectroscopic findings. The full occupation of the Ca(5) site in the β-TCP structure would correspond to $x = 0.286$. The rather high preparation temperature of 1000 °C apparently allows the substitution into further sites with larger CN and bond lengths: preferably Ca(1) with CN = 7 (≈ 2.4 Å) + 1 (≈ 3.0 Å) and/or Ca(2) with CN = 6 (≈ 2.4 Å) + 2 (≈ 2.7 Å). These sites have oxygen atoms with Ca(5) in common, which may well explain the mentioned discontinuity through geometric rearrangements between the interconnected polyhedra. EPR spectroscopy is indicative of such interconnections as well, where exchange narrowing along O–Mn–O bridgings occurs.

Finally, one might speculate about the improvement of biocompatibility of HA by Mn in light of these results. Possibly, the local formation of intermediary β-TCP phases plays a certain role in the respective mechanisms. As shown in this contribution, the phase effect becomes very distinct at higher concentrations of the manganese dopant.

Experimental Section

Synthesis of β-TCP from Mn-Containing HA Samples

Samples of HA with Mn (0.1–4.0%) and with carbonate (1.0–3.0%) and without carbonate were prepared by a precipitation method described in more detail elsewhere.[15] A phosphate solution [$(NH_4)_2HPO_4$ (3.7 g) in triple distilled water (TDW) (200 mL)] was added dropwise to a calcium solution [$Ca(NO_3)_2{\cdot}4H_2O$ (9.47 g) in TDW (200 mL)]. Carbonate (5.0 and 10.0 mL) was added from a $NaHCO_3$ stock solution (1 M). These additions were designed to give 2.5–3.5% carbonate in the final sample. The amount of Mn added was 0, 2.5, 5.0, 10, 15.0, 20.0, and 25.0 mL per sample from a $MnCl_2$ solution (0.025 M).

HA samples with Mn^{2+} were prepared at pH = 5.8–6.0. The pH was maintained constant during precipitation by addition of NaOH solution using a Mettler pH-stat automatic titrator. The precipitation was carried out over 2 h, and following this, the temp. was raised to the boiling point and the system was refluxed for 2 h. The sample was then washed with TDW and dried overnight in air at 120 °C.

The Ca, P, and Mn contents of the samples were determined by ICP-atomic emission spectroscopy with a precision of ±0.1, ±0.5, and ±0.3% for Ca, P, and Mn, respectively.

The subsequent heating, over 5 h, was carried out in porcelain crucibles in an electric furnace, from 600 °C to 1000 °C in 200 °C intervals.

Synthesis of β-TCP by High-Temperature Solid-State Reaction

Stoichiometric amounts of $CaCO_3$, $(NH_4)_2HPO_4$, and $Mn(NO_3)_2$ were thoroughly crushed and mixed in an agate mortar and heated in an alumina crucible at 300 °C for 3 h, recrushed, mixed and then heated at 1000 °C overnight. The samples with higher Mn content had a reddish-purple color.

Characterization Methods

XRD was used for crystal phase and lattice constant determination. The X-ray diffraction analyses were made by a Philips Automatic Diffractometer using Cu-K_α radiation. The samples were scanned in the 2θ range of 20–55°. The lattice parameters were calculated by a least-square computer program. Maximum deviation of the lattice constants was ±0.003 Å.

The characterization of the samples by infrared (IR) spectroscopy was performed by a Nicolet FTIR spectrometer. Samples (approx. 1 mg) were pressed into pellets with KBr (approx. 150 mg). The carbonate content of the samples was estimated by IR analysis using the extinction ratio of the carbonate (1420 cm^{-1}) and phosphate (575 cm^{-1}) bands. Carbonate is determined by this method with an accuracy of ±5%.[16]

EPR measurements were performed at X- and Q-band frequencies between 300 and 80 K with a Bruker ESP-300 spectrometer. UV/Vis spectra were recorded using the powder diffuse reflection technique with a Zeiss PMQII.

Samples were also examined by TEM. For this purpose they were ground and sonicated in ethanol. The obtained suspension was deposited onto a honeycomb carbon-coated grid. All of the study was done using the transmission electron microscope Tecnai F20 G^2 (FEI Company) operated at 200 kV and equipped with STEM HAADF detector and EDAX EDS detector.

[1] M. Vallet-Regi, *J. Chem. Soc., Dalton Trans.* **2001**, 97–108.
[2] A. Ogose, T. Hotta, H. Kawashima, N. Kondo, W. Gu, T. Kamura, N. Endo, *J. Biomed. Mater. Res., Part B, Appl. Biomater.* **2005**, *72*, 94–101.
[3] M. Aizawa, K. Itatani, I. Okada, *J. Ceram. Soc. Japan* **2005**, *113*, 245–251.
[4] A. Bigi, E. Foresti, M. Gazzano, A. Ripamonti, N. Roveri, *J. Chem. Research (S)* **1986**, 170–171.
[5] E. Jallot, J. L. Irigaray, H. Quadadesse, V. Brun, G. Weber, P. Frayssiner, *Eur. Phys. J. Appl. Phys.* **1999**, *6*, 205–215.
[6] I. Mayer, O. Jacobsohn, T. Niazov, J. Werckman, M. Iliescu, M. Richard-Plouet, O. Burghaus, D. Reinen, *Eur. J. Inorg. Chem.* **2003**, 1445–1451.
[7] A. Armulik, G. Svineng, K. Wennerberg, R. Faessler, S. Johansson, *Experimental Cell Res.* **2000**, *254*, 55–63.
[8] A. Bigi, B. Bracci, F. Cuisinier, R. Elkaim, M. Fini, I. Mayer, I. N. Mihailescu, G. Socol, L. Sturba, P. Torricelli, *Biomaterials* **2005**, *26*, 2381–2389.
[9] International Centre for Diffraction Data. Powder Diffraction File **2000**, 09–0432.
[10] International Centre for Diffraction Data. Powder Diffraction File **2001**, 09–0169 (2001).
[11] B. Dickens, L. W. Schroeder, W. E. Brown, *J. Solid State Chem.* **1974**, *10*, 232–248.
[12] F. E. Mabbs, D. Collison, in *Studies in Inorganic Chemistry* vol. 16 (Electron Paramagnetic Resonance of d Transition Metal Compounds), Elsevier, **1992**.
[13] D. Reinen, G. Schwab, W. Günzler, *Z. Anorg. Allg. Chem.* **1984**, *516*, 140–152.
[14] D. Reinen, H. Lachwa, R. Allmann, *Z. Anorg. Allg. Chem.* **1986**, *542*, 71–88; D. Reinen, W. Rauw, U. Kesper, M. Atanasov, H. U. Güdel, M. Hazenkamp, U. Oetliker, *J. Alloys Comp.* **1997**, *246*, 193–208.
[15] J. D. B. Featherstone, I. Mayer, F. C. M. Driessens, R. M. H. Verbeeck, M. Heijligers, *Calcif. Tissue Int.* **1983**, *35*, 169–171.
[16] J. D. B. Featherstone, S. Pearson, R. Z. LeGeros, *Caries Res.* **1984**, *18*, 63.

Received: November 14, 2005
Published Online: February 15, 2006

